

## Generation of an $S(\alpha, \beta)$ Covariance Matrix by Monte Carlo Sampling of the Phonon Frequency Spectrum

J.C. Holmes<sup>1</sup> and A.I. Hawari<sup>1,\*</sup>

<sup>1</sup>Department of Nuclear Engineering, North Carolina State University, Raleigh, NC 27695-7909, USA

Formats and procedures are currently established for representing covariances in the ENDF library for many reaction types. However, no standard exists for thermal neutron inelastic scattering cross section covariance data. These cross sections depend on the material's dynamic structure factor, or  $S(\alpha, \beta)$ . The structure factor is a function of the phonon density of states (DOS). Published ENDF thermal neutron scattering libraries are commonly produced by modeling codes, such as NJOY/LEAPR, which utilize the DOS as the fundamental input and directly output the  $S(\alpha, \beta)$  matrix. To calculate covariances for the computed  $S(\alpha, \beta)$  data, information about uncertainties in the DOS is required. The DOS may be viewed as a probability distribution function of available atomic vibrational energy states in a solid. In this work, density functional theory and lattice dynamics in the harmonic approximation were used to simulate the structure of silicon dioxide ( $\alpha$ -quartz) to produce the DOS. A range for the variation in the partial DOS for silicon in  $\alpha$ -quartz was established based on limits of variation in the crystal lattice parameters. Uncertainty in an experimentally derived DOS may also be incorporated with the same methodology. A description of possible variation in the DOS allowed Monte Carlo generation of a set of perturbed DOS spectra which were sampled to produce the  $S(\alpha, \beta)$  covariance matrix for scattering with silicon in  $\alpha$ -quartz. With appropriate sensitivity matrices, it is shown that the  $S(\alpha, \beta)$  covariance matrix can be propagated to generate covariance matrices for integrated cross sections, secondary energy distributions, and coupled energy-angle distributions.

### I. INTRODUCTION

Nuclear data libraries in ENDF-6 [1] format provide fundamental reaction information that is processed for use by modeling and simulation codes such as MCNP and SCALE. Uncertainties in the outputs of these codes are inherently functions of uncertainties and covariances in the ENDF library. ENDF formats and procedures are currently established for representing covariance matrices for various experiment-based nuclear data. These matrices are generated utilizing experimental and empirical model data. However, thermal neutron scattering libraries accounting for crystal structure are conventionally generated theoretically using atomistic models of the material of interest. In solids, these models can produce the phonon density of states (DOS) that defines the scattering law, or  $S(\alpha, \beta)$ . In this case, the DOS uncertainties are due to uncertainties in the atomistic simulation process. The DOS may be recognized as a probability distribution function of available energy states for energy exchange between a neutron and the atomic matrix. Consequently, by using a random sampling approach for

capturing the DOS uncertainties, the  $S(\alpha, \beta)$  covariance matrix can be established. This facilitates the construction of covariance matrices for differential and integral thermal inelastic scattering cross sections.

### II. CALCULATING UNCERTAINTY IN THERMAL INELASTIC SCATTERING

#### A. Scattering Theory

Thermal neutron inelastic scattering occurs through discrete emission and absorption of phonons which can be described as wave vectors in reciprocal space. If coherent inelastic scattering is negligible, as is the case for many materials (including  $\alpha$ -quartz), an incoherent approximation is valid. The double-differential inelastic thermal neutron scattering cross section in the incoherent approximation (as used by LEAPR [2]), in terms of the symmetric ENDF  $S(\alpha, \beta)$  dynamic structure factor, is

$$\frac{d^2\sigma(E)}{d\mu dE'} = \frac{\sigma_b}{2k_B T} \sqrt{\frac{E'}{E}} e^{-\beta/2} S(\alpha, \beta). \quad (1)$$

$E$  and  $E'$  are the incident and scattered neutron energies,  $\mu$  is the scattering angle cosine in the laboratory frame,

\* Corresponding author: [ayman.hawari@ncsu.edu](mailto:ayman.hawari@ncsu.edu)

$\sigma_b$  is the scattering nuclide bound cross section,  $k_B$  is Boltzmann's constant, and  $T$  is the temperature. The dimensionless momentum and energy transfer factors are  $\alpha = (E' + E - 2\sqrt{EE'\mu})/Ak_B T$  and  $\beta = (E' - E)/k_B T$ , respectively, where  $A$  is the scattering nuclide to neutron mass ratio. It is instructive to rewrite Eq. (1) as

$$\frac{d^2\sigma(E)}{d\alpha d\beta} = \frac{Ak_B T \sigma_b}{4E} e^{-\beta/2} S(\alpha, \beta). \quad (2)$$

In the incoherent approximation, the symmetric ENDF dynamic structure factor for one-phonon scattering is

$$S_1(\alpha, \beta) = \alpha e^{-\alpha\lambda} \frac{\rho(\beta)}{2\beta \sinh(\beta/2)}, \quad (3)$$

where

$$\lambda = \int_{-\infty}^{\infty} \frac{e^{-\beta/2} \rho(\beta)}{2\beta \sinh(\beta/2)} d\beta, \quad (4)$$

is the Debye-Waller coefficient. The term  $\rho(\beta)$  is the phonon DOS in terms of  $\beta$ , and

$$S(\alpha, \beta) = \sum_{n=1}^{\infty} S_n(\alpha, \beta), \quad (5)$$

where  $S_n(\alpha, \beta)$  are the terms for  $n$ -phonon scattering. These are calculated by successive convolutions over  $\rho(\beta)$  [2]. As such, the higher-order terms are progressively less sensitive to the features of  $\rho(\beta)$ . However, as  $E \rightarrow 0$  (and as  $\alpha \rightarrow 0$ ), one-phonon scattering becomes increasingly dominant.

### B. Covariance Matrices

The general matrix formula for first order propagation of uncertainty is

$$\mathbf{V}_y = \mathbf{M}^T \mathbf{V}_x \mathbf{M}. \quad (6)$$

$\mathbf{V}_x$  and  $\mathbf{V}_y$  are the covariance matrices for all input variables  $x$  and all output variables  $y$ . Define  $x$  as the set of all  $S(\alpha, \beta)$  terms, calculated over  $\alpha$  and  $\beta$  grids, and define  $y$  as a data set resulting from integrating Eq. ((2)) over specified ranges of  $\alpha$  and/or  $\beta$ . For given  $T$ ,  $A$  and  $E$ , only  $S(\alpha, \beta)$  for physically possible  $\alpha$  and  $\beta$  combinations can be included in the integration.  $\mathbf{M}$  is the sensitivity matrix for each  $y$  variable with respect to each  $x$  variable, with entries  $\mathbf{M}_{ij} = \partial y_j / \partial x_i$ . Since numerical integration of  $S(\alpha, \beta)$  over  $\alpha$  and/or  $\beta$  grids is analogous to algebraic summing,  $\mathbf{M}$  is trivial to construct. Given  $\mathbf{V}_x$  for  $S(\alpha, \beta)$ , it is straightforward in principle to construct  $\mathbf{V}_y$  for any integrated output data set [3]. These may include  $\sigma(E)$ ,  $d\sigma(E)/dE'$ , or coupled energy-angle distributions. To theoretically calculate a dynamic structure factor covariance matrix, a description of uncertainties in the DOS is required.

### III. ASSESSING UNCERTAINTY IN THE PHONON FREQUENCY SPECTRUM

The DOS can be generated using the *ab initio* code VASP and lattice dynamics code PHONON [4–6]. Model parameters are supplied to VASP, including crystal structure and lattice constants. VASP relaxes the system to its lowest energy state and calculates Hellmann-Feynman forces between atoms. Applying lattice dynamics in the harmonic approximation, PHONON constructs a dynamical matrix using the forces calculated by VASP. Through random sampling of wave-vectors (and their associated phonon frequency eigenvalues) in the first Brillouin zone, the DOS is produced pointwise over a specified energy mesh. This can then be renormalized to generate  $\rho(\beta)$ . Thus,  $\rho(\beta)$  is a probability distribution function of available excitation energy states defined over discrete bins and scaled by  $k_B T$ .

The features of this calculated  $\rho(\beta)$  may be offset to some extent in energy or have some error in magnitude with respect to the true  $\rho(\beta)$ . Calculated values at each energy point are already statistical averages over the energy resolution established for the wave-vector sampling. Additional uncertainties exist due to uncertainties in model parameters and/or the model itself. Determining this explicitly would be cumbersome. However, by varying the lattice constants supplied to VASP over the range of experimental to relaxed values (<1% change), and by testing the sensitivity of  $\rho(\beta)$  to other model parameters in the input of VASP, an expected maximum variation in the features of  $\rho(\beta)$  can be assessed. The  $\rho(\beta)$  spectrum can be randomly perturbed within the observed range of variation, while accounting for statistical uncertainty and keeping features appropriately coupled in energy, to produce a set of renormalized perturbed  $\rho(\beta)$  spectra. A full  $S(\alpha, \beta)$  matrix can be calculated from each  $\rho(\beta)$  in this set. Each calculation consists of one Monte Carlo trial. An  $S(\alpha, \beta)$  covariance matrix may then be calculated by processing the results of a large number of trials.

### IV. MONTE CARLO RESULTS

For this work, Si in  $\text{SiO}_2(\alpha\text{-quartz})$  was selected as the scattering medium to demonstrate the impact of particular characteristics of its DOS. Fig. 1 gives the reference  $\rho(\beta)$  spectrum for Si in  $\alpha\text{-quartz}$  [7]. The spectrum was observed to shift up to a maximum of about 1 meV, or slightly more than one bin width, although not uniformly over energy. For each of the 500 Monte Carlo trials performed, the random perturbations in  $\rho(\beta)$  account for this localized energy-shift potential. To benefit the instructive quality of the  $S(\alpha, \beta)$  results, a moderately low fixed  $\alpha = 0.1$  is used which ensures significant one-phonon scattering while not overly suppressing multiphonon scattering. For all cases,  $T = 293.6\text{K}$  is the reference temperature. For clarity, the abscissa for all plots is in energy

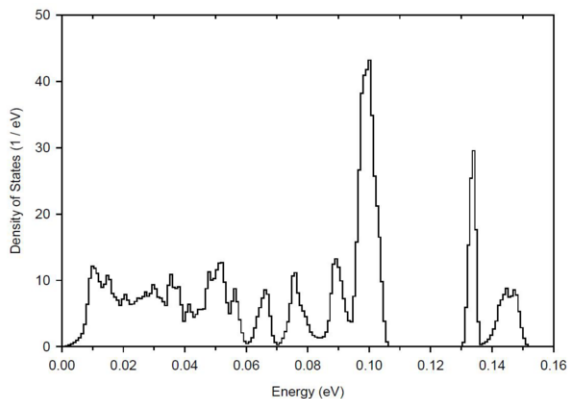


FIG. 1.  $\rho(\beta)$  for Si in  $\alpha$ -quartz plotted over energy (eV).

(eV) instead of  $\beta$ .

$S(\alpha, \beta)$  was calculated to phonon order 8 (which is sufficient for convergence for  $\alpha = 0.1$ ) over a fixed  $\beta$  grid. For each Monte Carlo trial, in addition to  $\rho(\beta)$  spectral shifting, a temperature uncertainty of 1% was instituted (where 1% is considered one standard deviation for a normal distribution with mean  $T = 293.6K$ ). Since  $\beta$  is a function of temperature, the  $\beta$  grid points at which  $S(\alpha, \beta)$  is calculated are scaled by  $T_{random}/T_{reference}$  for each Monte Carlo trial. This allows plotting uncertainty in  $S(\alpha, \beta)$  as a function of energy transfer. Fig. 2 gives  $-1\sigma$  and  $+1\sigma$  bands for  $S(\alpha, \beta)$  about its mean to display the range of variation.

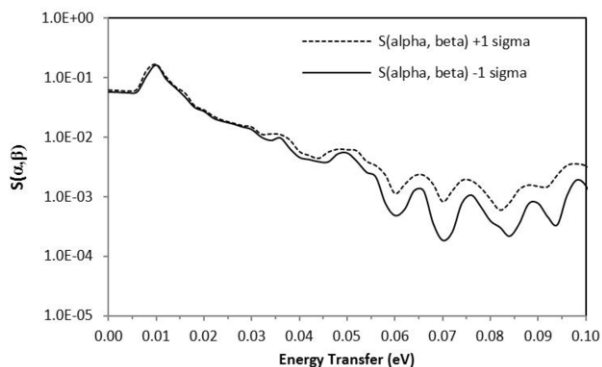


FIG. 2. ENDF  $S(\alpha, \beta)$  high and low bands for  $\pm \sigma$ .

The percent standard error in  $S(\alpha, \beta)$  with and without the 1% temperature variation is demonstrated in Fig. 3. Multiphonon scattering increases with temperature as the phonon occupation number rises. Therefore, when the 1% temperature variation is introduced, peaks in uncertainty are seen at energy transfers where one-phonon scattering, or  $\rho(\beta)$ , has low probability (e.g., 0.06, 0.07, 0.085 and 0.095 eV) and valleys are seen at energy transfers where one-phonon scattering is dominant (e.g., 0.065, 0.075 and 0.09 eV). For the case without temperature variation, peaks in uncertainty are seen at energy transfers associated with high-slope regions of  $\rho(\beta)$  (e.g., 0.062, 0.068 and 0.072 eV) and valleys are seen at energy transfers

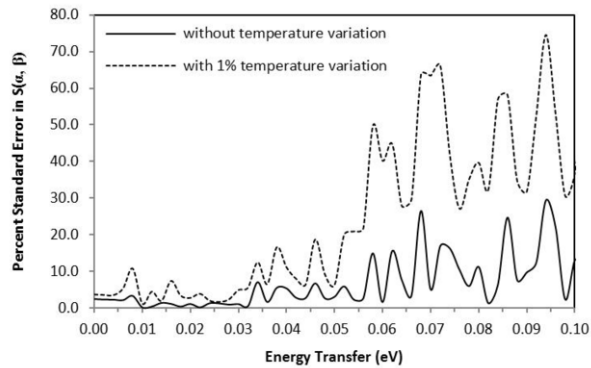


FIG. 3. ENDF  $S(\alpha, \beta)$  percent standard error with and without temperature variation.

associated with flatter regions of  $\rho(\beta)$  (e.g., 0.06, 0.065 and 0.07 eV).

Fig. 4 separates the percent standard error in  $S(\alpha, \beta)$ , with no temperature variation, into one-phonon and multiphonon scattering components. It can be seen that

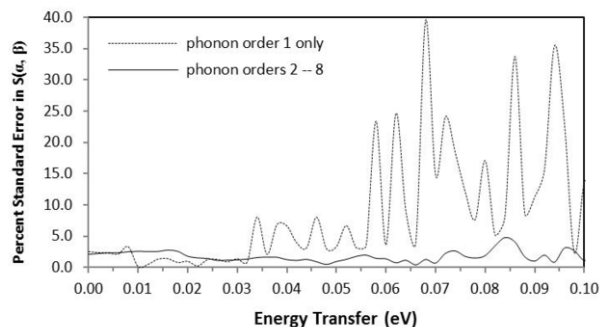


FIG. 4. ENDF  $S(\alpha, \beta)$  percent standard error, with no temperature variation, for one-phonon and multiphonon scattering.

most of the uncertainty introduced by randomly shifting  $\rho(\beta)$  in energy is exhibited through one-phonon scattering. This is because higher-order phonon terms, even when dominant, are largely insensitive to the structure of  $\rho(\beta)$ . At a particular energy transfer, the uncertainty for all-phonon scattering (as shown in Fig. 3) is less than the uncertainty for one-phonon scattering due to one-phonon and multiphonon scattering being negatively correlated.

Percent standard error in differential cross sections with respect to energy transfer (integrated over all physical  $\alpha$ ) is given in Fig. 5 with and without temperature variation. It is evident that the integrated uncertainties are smaller, but still significant. With temperature variation, there is greater uncertainty in upscattering (which has a larger multiphonon component) than in downscattering. Conversely, without temperature variation, there is greater uncertainty in downscattering (which has a larger one-phonon component) than in upscattering. In either case, the net percent standard error in integrated upscattering and downscattering cross sections is on the

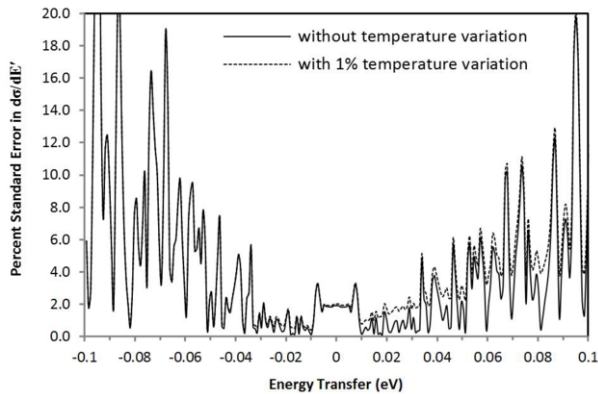


FIG. 5. Percent standard error in differential cross sections with respect to energy transfer, with and without temperature variation.

order of a few percent, even for the extremely small perturbations introduced in  $\rho(\beta)$  and in temperature.

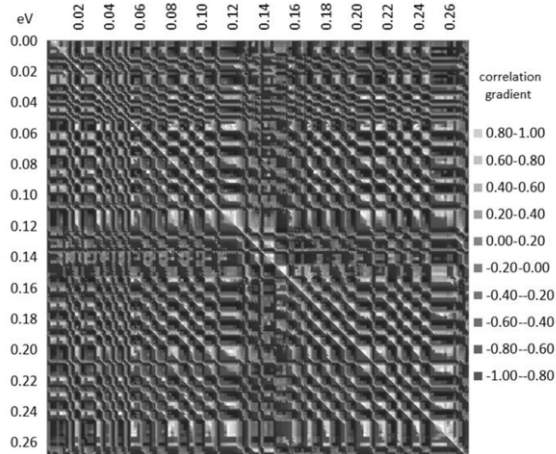


FIG. 6. Topographic map of the  $S(\alpha, \beta)$  correlation matrix.

It is instructive to view a cross section of the  $S(\alpha, \beta)$  correlation matrix vs. the covariance matrix. In the ex-

ample given in Fig. 6, temperature variation does not occur and  $\alpha = 0.1$ . The structure of  $\rho(\beta)$  is evident. The diagonal of full correlation is easily seen along with elevated bands associated with regions of  $\rho(\beta)$  with low probability (where highly correlated multiphonon scattering terms are present). The continuous relatively flat region of  $\rho(\beta)$  is evident below 0.06 eV, with relatively little correlation variation over energy. The axes extend to 0.27 eV, allowing correlation blocks to be seen which correspond to combinations of high probability regions of  $\rho(\beta)$  (e.g., 0.20 eV =  $2 \times 0.10$  eV). The ridges evident throughout generally map the features of  $\rho(\beta)$  over energy. While not displayed, the features of the  $S(\alpha, \beta)$  correlation matrix mapped over  $\alpha$  for fixed  $\beta$  are smooth and can be predicted analytically.

## V. CONCLUSIONS

A Monte Carlo method of sampling randomly perturbed phonon spectra to generate an  $S(\alpha, \beta)$  covariance matrix has been implemented. Among other factors, the quantification of the  $S(\alpha, \beta)$  covariance matrix depends on uncertainties in the phonon spectrum, which is a fundamental input to the scattering law. The phonon spectrum uncertainties were estimated as a function of variations in the atomistic model parameters. In this work, the  $S(\alpha, \beta)$  covariance matrix for Si in  $\alpha$ -quartz was propagated to calculate a covariance matrix for differential scattering cross sections with respect to energy transfer. It was found that a maximum 1% variation in the lattice constants resulted in maximum uncertainties of about 20% in these differential cross sections. It is anticipated that this methodology would enable the description of covariances in ENDF thermal neutron inelastic scattering data based on both computational analysis and experimental measurements.

*Acknowledgements:* This work is supported by U.S. DOE contract number 00042959. J.C. Holmes is supported by a DOE Nuclear Energy University Programs fellowship.

- 
- [1] The Cross Section Evaluation Working Group, ENDF-102, National Nuclear Data Center, Brookhaven National Laboratory, USA (2010).
  - [2] R.E. MacFarlane and D.W. Muir, Report LA-12740-M (1994).
  - [3] D.L. Smith, "Probability, Statistics, and Data Uncertainties in Nuclear Science and Technology," American Nuclear Society, LaGrange Park, IL, USA (1991).
  - [4] G. Kresse and J. Furthmuller, *COMP. MAT. SCIENCE* **6**, 15 (1996); *PHYS. REV. B* **54**, 11169 (1996).
  - [5] K. Parlinski *et al.*, *PHYS. REV. LETT.* **78**, 4063 (1997).
  - [6] A.I. Hawari *et al.*, *PHYSOR 2004*, Chicago, IL, USA (2004).
  - [7] B.D. Hehr and A.I. Hawari, *PHYSOR 2008*, Interlaken, Switzerland (2008).